Original Article

Feasibility of dual-phase ^{99m}Tc-MDP SPECT/CT imaging in rheumatoid arthritis evaluation

Yasser G. Abdelhafez[1,2]^, Felipe Godinez[1,3], Kanika Sood[4], Rosalie J. Hagge[1], Robert D. Boutin[1,5], Siba P. Raychaudhuri[4,6], Ramsey D. Badawi[1], Abhijit J. Chaudhari[1]

[1]Department of Radiology, University of California Davis, Sacramento, CA, USA; [2]Nuclear Medicine Unit, South Egypt Cancer Institute, Assiut University, Assiut, Egypt; [3]School of Biomedical Engineering and Imaging Science, King's College, London, UK; [4]Rheumatology Section, Sacramento Veterans Affairs Medical Center, Mather, CA, USA; [5]Department of Radiology, Stanford University, Stanford, CA, USA; [6]Department of Internal Medicine, University of California Davis, Sacramento, CA, USA

Correspondence to: Abhijit J. Chaudhari, PhD. Department of Radiology, University of California Davis, 4860 Y Street, Suite 3100, Sacramento, CA 95817, USA. Email: ajchaudhari@ucdavis.edu.

Background: To prospectively demonstrate the feasibility of performing dual-phase SPECT/CT for the assessment of the small joints of the hands of rheumatoid arthritis (RA) patients, and to evaluate the reliability of the quantitative and qualitative measures derived from the resulting images.

Methods: A SPECT/CT imaging protocol was developed in this pilot study to scan both hands simultaneously in participants with RA, in two phases of ^{99m}Tc-MDP radiotracer uptake, namely the soft-tissue blood pool phase (within 15 minutes after radiotracer injection) and osseous phase (after 3 hours). Joints were evaluated qualitatively (normal *vs.* abnormal uptake) and quantitatively [by measuring a newly developed metric, maximum corrected count ratio (MCCR)]. Qualitative and quantitative evaluations were repeated to assess reliability.

Results: Four participants completed seven studies (all four were imaged at baseline, and three of them at follow-up after 1-month of arthritis therapy). A total of 280 joints (20 per hand) were evaluated. The MCCR from soft-tissue phase scans was significantly higher for clinically abnormal joints compared to clinically normal ones; P<0.001, however the MCCR from the osseous phase scans were not different between the two joint groups. Intraclass Correlation Coefficient (ICC) for MCCR was excellent [0.9789, 95% confidence interval (CI): 0.9734–0.9833]. Intra-observer agreement for qualitative SPECT findings was substantial for both the soft-tissue phase (kappa =0.78, 95% CI: 0.72–0.83) and osseous-phase (kappa =0.70, 95% CI: 0.64–0.76) scans.

Conclusions: Extracting reliable quantitative and qualitative measures from dual-phase 99mTc-MDP SPECT/CT hand scans is feasible in RA patients. SPECT/CT may provide a unique means for assessing both synovitis and osseous involvement in RA joints using the same radiotracer injection.

Keywords: Bone scan; rheumatoid arthritis; SPECT/CT; soft tissue vascularity; osteoblastic response

Submitted Aug 24, 2020. Accepted for publication Dec 23, 2020.
doi: 10.21037/qims-20-996
View this article at: http://dx.doi.org/10.21037/qims-20-996

^ ORCID: 0000-0002-1989-3094.

© Quantitative Imaging in Medicine and Surgery. All rights reserved.

Introduction

Synovitis is the hallmark of Rheumatoid Arthritis (RA), and is typically characterized by leukocyte infiltration, hypervascularity, neoangiogenesis, synoviocyte proliferation and fibroblast activation (1). The inflamed synovial membrane may initiate and promote further invasion of cartilage and bone (2). Additionally, synovitis may stimulate osteoclastic differentiation with subsequent cortical bone resorption and breach of the synovium/bone marrow barrier (3). This has been designated as the outside-in hypothesis, in contrast to the inside-out hypothesis, which postulates that joint inflammation originates in the bone marrow (4). The changes in the status of synovial vascularity and bone metabolism are known to typically precede anatomical changes; therefore, non-invasive imaging tools capable of quantifying these processes may offer unique opportunity for RA disease activity evaluation and risk stratification (5).

Skeletal scintigraphy using diphosphonate radiotracers has been used for assessing inflammatory arthritis (6,7). Soft-tissue phase images acquired shortly after tracer injection reflects local blood flow and soft tissue vascularity, which typically are increased during inflammation (8); while the delayed osseous phase (3–4 h after injection) is reflective of osteoblastic response (9).

Most of the published studies to date employing scintigraphy in RA patients used a single delayed osseous phase scan, in planar, two-dimensional acquisition mode (10,11). Only a few studies have utilized scanning at multiple timepoints (12) or used three-dimensional acquisition techniques (13-15). The acquisition of dual-phase SPECT/CT could provide insight into RA disease activity in the small joints. However, there is concern that the spatial and contrast resolution afforded by SPECT/CT may not be adequate for scanning of the small joints, such as those of the wrist and hand, that are affected earlier in the RA disease process.

The purpose of this pilot study was to prospectively demonstrate the feasibility of performing dual-phase SPECT/CT for the assessment of the small joints of the hands of rheumatoid arthritis (RA) patients, and to evaluate the reliability of the quantitative and qualitative measures derived from the resulting images.

Methods

Study participants

This pilot study was approved by the Institutional Review Board of the University of California Davis. Written informed consent was obtained from all study participants. The study recruited participants with established rheumatoid arthritis (RA) based on the American College of Rheumatology (ACR) 2010 criteria (16), and who were candidates for starting treatment with first-line disease modifying anti-rheumatic (DMARDs) drugs (N=3) or tumor necrosis factor-alpha (TNF-α) blockers (N=1). SPECT/CT scans were conducted at baseline before starting treatment, and again at one month after therapy. Scan timing during the day, waiting interval, positioning and hydration status were matched between the two timepoints. The early soft-tissue phase scans were scheduled for late morning or early afternoon to mitigate the impact of morning stiffness. Waiting interval was kept between 3–4 hours. Participants were provided hydration instructions as part of study preparation and screening for hydration status was part of the routine workup. Drug response was assessed by a board-certified rheumatologist using the ACR 20 criteria (16). Additionally, disease activity score for 28 joints (DAS-28) (17) was recorded at baseline and after 6 months from baseline scans.

SPECT/CT imaging protocol development

All SPECT/CT images were acquired using Philips BrightView XCT (Philips Healthcare, Cleveland, OH) equipped with low-energy all-purpose (LEAP) collimator. Our first step was to develop means to standardize the position of participant's body on the scanner bed such that the hands can extend to fall within the field of view (FOV) of gamma cameras; to minimize photon attenuation and maximize coverage. To achieve this task, we designed an immobilization device (*Figure 1*) made of 2 low-attenuation detachable hand-shaped thermoplastic molds mounted to acrylic plates using low-density plastic screws. The top edges of the two plates meet at the midline and the front edges converge distally to match the natural orientation of the outstretched hands. The detachable plates are secured by docking them via grooves on a wooden base, that hangs off the edge of the bed, such that it runs for a length of 120 cm under the bed cushion. The participant's weight provides stability to the assembly (*Figure 1*).

Next, we evaluated a range of SPECT image reconstruction schemes using a phantom with fillable spheres with varying sizes, that approximately match the sizes of the hand joints, with the goal of obtaining high quantitative reproducibility and contrast-to-noise ratio

© Quantitative Imaging in Medicine and Surgery. All rights reserved.

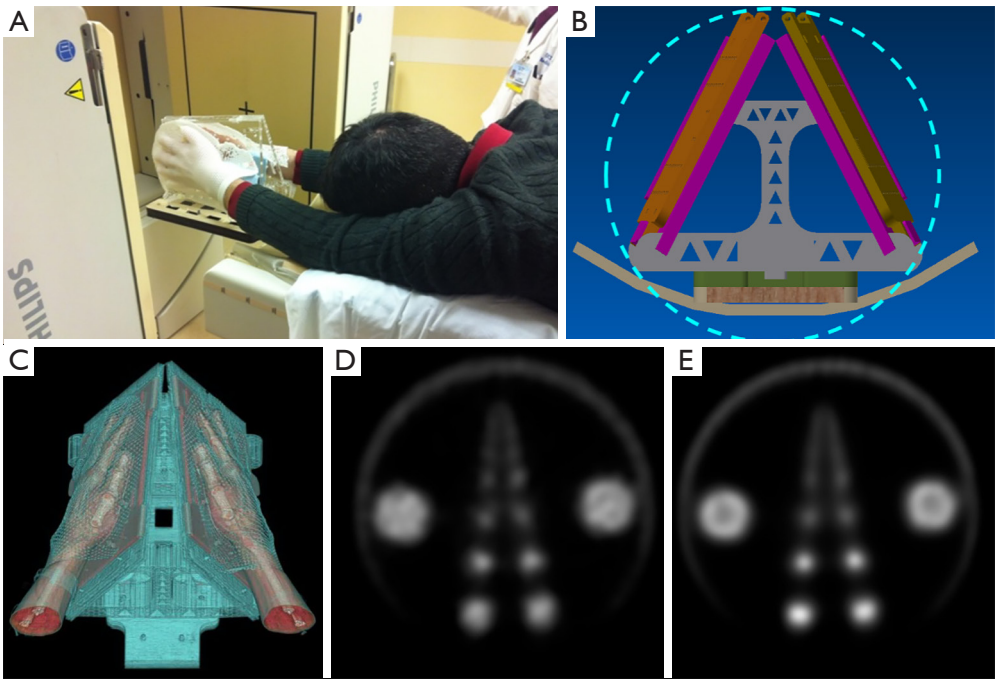

Figure 1 SPECT/CT imaging protocol development. (A,B,C) The immobilization device. (A) Participant position with their hands, inside the immobilizer, outstretched over the shoulders in superman position. (B) Design drawing, showing that a circular gamma camera data acquisition trajectory (light blue line) is feasible. (C) 3D rendering generated from CT scans of a participant in our pilot study, showing that the base station allows for maintenance of the natural angles of the arms during scanning. (D,E) Comparison of image reconstruction schemes, with OSEM (D) and OSEM with PSF correction (E). The largest spheres are of diameter 3.8 cm and show the characteristic ring-like artifact on (E), however, the contrast for smaller spheres (2.2 cm and below) is improved. SPECT/CT, single photon emission computed tomography/computed tomography; OSEM, ordered subset expectation maximization; PSF, point spread function

despite the small size of the joints of the wrist and hand.

Overall, our acquisition protocol converged on these acquisition parameters: 64 frames (32 per head), 20 seconds/frame (total ~11 minutes), zoom 1.46 and matrix size 128×128 pixels. With these acquisition parameters, we compared the performance of the iterative ordered subset expectation maximization (OSEM) method and the OSEM method with point spread function (PSF) correction (*Figure 1*). We evaluated the reconstructed image properties such as contrast-recovery-coefficient, image uniformity, and the bias-variance trade-off. Accordingly, we selected the OSEM method with PSF correction (4 iterations, 16 subsets), incorporating both attenuation and scatter correction. The reconstructed image slice thickness for SPECT was 3.19 mm while that for CT was 1.0 mm.

SPECT/CT image acquisition and analysis

Dual-phase scans were acquired starting at 5 min (soft-tissue phase) and 180 min (osseous phase) following a single intravenous injection of 963±36 MBq of ^{99m}Tc-MDP. A low-dose CT was acquired for the same field of view after each SPECT scan using an integrated cone-beam x-ray source and a flat-panel detector (tube current: 20 mA; voltage: 120 kVp). The calculated additional radiation dose due to low-dose CT was 0.2 mSv. The total scan time (SPECT+CT) for each phase was 15 min. Participants were allowed to resume their normal activity during the interval between the 5- and 180-min scans.

The reconstructed images were reviewed by one nuclear medicine physician with 15 years of experience on a workstation running OsiriX MD v.8.0 (Pixmeo, Brenex, Switzerland). Twenty joints per hand were assessed [wrist, carpometacarpal (CMC), metacarpophalangeal (MCP), proximal and distal interphalangeal (PIP & DIP)]. The wrist joint was considered as a single entity. Images were evaluated qualitatively (visual assessment) and quantitatively. Visual assessment described the signal intensity using a

© Quantitative Imaging in Medicine and Surgery. All rights reserved.

Table 1 Clinical characteristics of the study participants

Characteristic	Participant 1	Participant 2	Participant 3	Participant 4
Age (years)	74	70	56	65
Antibody status	Seropositive	Seronegative	Seronegative	Seronegative
Clinically abnormal joints	7	0	2	2
Baseline DAS-28	3.65	0.7	3.06	2.43
Baseline CRP	14	0.7	16	1.2
Treatments	MTX	SSZ, Prednisone, Hydroxurea	SSZ	Etanercept
DAS-28 at 6 months	2.33	1.11	1.99	2.43
Final status	Responder	Responder	Non-responder	Non-responder

MTX, methotrexate; SSZ, Sulfasalazine; DAS-28, disease-activity score for 28 joints; CRP, C-reactive protein.

subjective 4-point scale commonly reported in practice (no/mild/moderate/marked uptake). During data analysis, the first two categories were considered within normal and the latter two (moderate or marked uptake) were considered abnormal.

To quantify tracer uptake, a volume of interest (VOI) was drawn on each of the 20 joints based on the low-dose CT images, and the maximum count values were recorded from the corresponding co-registered SPECT images after checking for any mis-registration. Values from all the joints that were both clinically and scintigraphically normal/unremarkable were averaged. The ratio of the maximum count value in each joint normalized by this average, termed maximum corrected count ratio (MCCR), was computed.

For subset analysis, the 11 joints known to be more frequently affected by RA; which included 1st–5th MCPs, 2nd–4th PIPs, 1st IP and wrist joints; were classified as Group I. The rest of the joints (n=9 per hand), including 1st–5th CMC and 2nd–4th DIP joints, were classified as Group II.

To ensure consistency and reproducibility, each of the two SPECT phases were reviewed on separate days; also, all the qualitative and quantitative readings were repeated after at least 3-month interval, on the same viewing workstation by the same reader to quantify intra-observer agreement.

Statistical analysis

Qualitative data were expressed as frequencies and percentages. Association between categorical variables was compared using chi-square test for independent variables or Spearman's rank correlation, as appropriate. Quantitative data were summarized and expressed as median (range). Two-tailed Mann-Whitney U or Wilcoxon rank tests were used for comparing two independent or related groups; respectively. Intra-reader agreement was measured using kappa statistic for qualitative observations and intraclass correlation coefficient (ICC) for quantitative variables. Differences in paired readings were measured using McNemar's test.

Results

Study participants

Between May 2015 and May 2016, four participants (all males; median age 67.5 years, range: 53–74) were recruited for this pilot study. Their clinical characteristics are summarized in *Table 1*. Three participants successfully completed the two scans (at the baseline and 1-month follow-up), while one participant completed only the baseline scan. No participants were excluded due to non-compliance with the protocol. During each visit, SPECT/CT scans during the two phases of radiotracer uptake were successfully completed. No visual evidence of intra-scan motion artifacts was detected in any of the acquired images (4 participants, 7 studies with a total of 14 SPECT/CT scans and 280 joints evaluated).

Qualitative and quantitative SPECT/CT findings

Among the total 280 joints evaluated, 22 joints (16 in Group I and 6 in Group II) were clinically abnormal. SPECT imaging showed abnormally increased tracer uptake during both soft-tissue and osseous phases in 10 joints, all from Group I. However, soft-tissue and osseous-phase SPECT

© Quantitative Imaging in Medicine and Surgery. All rights reserved.

showed additional abnormality in 72 (31 Group I, 41 Group II) and 92 (44 Group I, 48 Group II) joints, respectively, that did not present with obvious clinical findings. The pattern of abnormal radiotracer uptake within the same joint was notably different between the soft-tissue and osseous phases (*Figure 2*).

Quantitatively, the mean MCCR from soft-tissue phase SPECT was significantly higher for clinically abnormal joints (2.50±1.68) compared to clinically normal ones (1.35±0.79; P<0.0001). Such differences were not seen with the osseous phase SPECT assessments, which showed a median MCCR of 1.76±1.21 and 1.34±0.71 for clinically abnormal and normal joints, respectively.

MCCR demonstrated significant positive correlation with the 4-point visual score of uptake intensity, with Spearman's rank correlation coefficients of 0.78 (95% CI: 0.73–0.82) and 0.84 (95% CI: 0.8–0.87) for the soft-tissue and osseous-phase SPECTs, respectively. Qualitative and quantitative SPECT findings are summarized in *Table 2*.

Agreement between soft-tissue and osseous phases

Soft-tissue MCCR showed moderate positive correlation with osseous-phase MCCR (r=0.64, 95% CI: 0.56–0.70; P<0.001). Visually, the presence of soft-tissue hypervascularity was not accompanied with osseous uptake in 17/82 joints (8 from Group I, 9 from Group II). Conversely, 37/102 joints with high osseous uptake did not demonstrate hypervascularity (21 from Group I, 16 from Group II). That discordance between the soft-tissue and osseous phases was more evident within Group I (P=0.03) compared to Group II joints (P=0.2).

Observer agreement

MCCR was highly reliable (ICC >0.995) when a repeated measurement was performed (*Table 3*). Intra-observer agreement on the qualitative SPECT findings was substantial for all joints, both from soft-tissue and osseous phases (*Table 3*).

Relation of quantitative SPECT to response

Group I joints showed higher MCCR from baseline soft-tissue phase SPECT scans (*Table 4*) in non-responders compared to responders (1.65 *vs.* 1.31). Similarly, a slightly higher MCCR from baseline delayed osseous phase SPECT scans was noted in non-responders compared to responders (1.25 *vs.* 1.19; *Table 4*; *Figure 2*).

Interestingly, Group II joints (osteoarthritis) showed slightly increasing soft-tissue phase MCCR in responders.

Discussion

In RA a quantitative understanding of synovial vascularity and altered bone metabolism may provide means for robustly assessing disease activity before irreversible anatomical damage is manifested (5,18). In this prospective pilot study, we demonstrated the feasibility and reliability of measuring markers corresponding to synovitis and bone metabolism in small joints of an RA cohort using dual-phase SPECT/CT scanning. Our rationale is that SPECT/CT scans, due to their inherent 3D nature, eliminate the superimposition problem of planar imaging, and therefore improve the sensitivity, specificity and spatial resolution compared to planar scintigraphy (19).

Previous studies designed a specialized multi-pinhole high resolution collimator for use in animal models (14) and RA patients (13,15,20). Multi-pinhole SPECT cameras provide significantly higher sensitivity and resolution compared to parallel-hole collimators, but typically have a vastly limited field of view (10 or 20 cm depends on aperture design), which limits the scans to the fingers or wrist of one hand at a time. SPECT scans using this approach were able to detect a larger number of diseased joints compared to planar imaging. Also, investigators accurately localized the exact sub-region of the joint that showed increased uptake. However, studies performed using such cameras to date employed only the single delayed osseous phase SPECT scanning for the most clinically affected hand. That may represent a particular limitation for RA assessment, as RA is typically bilateral and often symmetric disease. Also, software fusion with other cross-sectional images is challenging. Hybrid SPECT/CT machines have the advantages of hardware fusion of the functional tracer distribution and anatomical information in three dimensions, which allows accurate registration, attenuation correction and potential for assessment of CT changes within the small joints (21). The added radiation dose from the low-dose CT is typically not significant. With newer SPECT/CT machines, calculation of Standardized Uptake Values (SUV) is feasible and could further enhance quantitative assessment (22,23).

Our results demonstrated that, quantitatively, the tracer activity from soft-tissue uptake (indicative of vascularity) was significantly higher in clinically positive joints. On the other

© Quantitative Imaging in Medicine and Surgery. All rights reserved.

Figure 2 SPECT/CT images of a 74-year-old patient with seropositive RA at the baseline (top; A,B,C,D,E) and one-month (bottom; F,G,H,I,J) after therapy: volume rendered maximum intensity projection (MIP) of the fused SPECT/CT images of the left hand (A,C,F,H) and magnified SPECT/CT images of the 2nd finger PIP joint (arrow; B,D,G,I) in sagittal (top), coronal (middle) and axial (bottom) projections, with the corresponding low-dose CT (E,J). Baseline soft-tissue SPECT/CT (A) demonstrates hypervascularity in 1st IP & CMC, 2nd, 3rd & 5th PIP joints, with nearly circumferential hypervascularity pattern around the 2nd PIP (B). Corresponding MIP from the osseous SPECT/CT phase (C) showing increased osseous turnover in the 2nd and 5th PIP regions with asymmetric tracer distribution across the joint. The uptake is more prominent on the radial aspect of the distal end of the proximal phalanx of the 2nd PIP (D). The corresponding low-dose CT images (E) show no evidence of erosive changes. The follow-up images (F-J) demonstrate significant improvement of the previously noted hypervascularity of the affected joints (F). Second PIP joint images (G) demonstrate the most striking changes in tracer intensity and distribution. The osseous phase images (H, I) also demonstrate reduction of tracer uptake, but still eccentric and radially located. There was no clear evidence of erosions on the low-dose CT (J). SPECT/CT, single photon emission computed tomography/computed tomography; RA, rheumatoid arthritis; MIP, maximum intensity projection; PIP, proximal interphalangeal; IP, interphalangeal; CMC, carpo-metacarpal.

© Quantitative Imaging in Medicine and Surgery. All rights reserved.

Table 2 Qualitative and quantitative SPECT findings in different joint groups

Joint group	Visual assessment	Median MCCR (range)	
		Soft tissue	Osseous
2nd–5th MCPs	Normal	0.90 (0.37–1.82)	0.92 (0.43–1.30)
	Abnormal	1.66 (1.25–1.90)	1.88 (1.37–2.70)
2nd–5th PIPs	Normal	1.02 (0.40–2.80)	1.00 (0.60–1.72)
	Abnormal	2.18 (1.26–6.30)	1.63 (1.20–5.87)
2nd–5th DIPs	Normal	1.22 (0.80–3.20)	1.10 (0.70–1.53)
	Abnormal	1.80 (1.23–3.90)	1.83 (1.22–6.14)
2nd–5th CMCs	Normal	0.82 (0.39–1.48)	0.98 (0.54–1.70)
	Abnormal	1.80 (1.60–1.99)	1.40 (1.24–1.50)

MCCR, maximum corrected count ratio; MCPs, metacarpophalangeal joints; PIPs, proximal inter-phalangeal joints; DIPs, distal inter-phalangeal joints; CMCs, carpo-metacarpophalangeal joints.

Table 3 Intra-observer agreement on qualitative and quantitative evaluations of the different joints from dual-phase ^{99m}Tc-MDP SPECT/CT of the hands

Joints	N	Soft-tissue phase		Osseous phase	
		Kappa (95% CI)	ICC (95% CI)	Kappa (95% CI)	ICC (95% CI)
All	280	0.777 (0.723–0.830)	0.979 (0.973–0.983)	0.700 (0.642–0.759)	0.979 (0.973–0.983)
Group I	154	0.799 (0.729–0.868)	0.980 (0.973–0.985)	0.762 (0.690–0.835)	0.993 (0.990–0.995)
2nd–5th PIPs	56	0.803 (0.694–0.912)	0.979 (0.964–0.988)	0.720 (0.603–0.837)	0.994 (0.990–0.997)
2nd–5th MCPs	56	0.799 (0.652–0.945)	0.966 (0.943–0.980)	0.795 (0.668–0.922)	0.988 (0.980–0.993)
Group II	126	0.747 (0.664–0.830)	0.977 (0.967–0.984)	0.626 (0.532–0.719)	0.993 (0.991–0.995)
2nd–5th DIPs	56	0.665 (0.516–0.814)	0.970 (0.949–0.982)	0.568 (0.440–0.696)	0.992 (0.986–0.995)
2nd–5th CMCs	56	0.629 (0.431–0.828)	0.960 (0.932–0.976)	0.423 (0.231–0.616)	0.976 (0.959–0.986)
1st CMCs	14	0.779 (0.556–1.000)	0.958 (0.876–0.987)	0.853 (0.651–1.000)	0.996 (0.987–0.999)

ICC, intraclass correlation coefficient; CI, confidence interval; MCPs, metacarpophalangeal joints; PIPs, proximal inter-phalangeal joints; DIPs, distal inter-phalangeal joints; CMCs, carpo-metacarpophalangeal joints.

Table 4 Maximum corrected count ratio (MCCR) at the baseline and 1-month after therapy for group I (rheumatoid arthritis) and Group II (osteoarthritis) joints in responder and non-responder participants. Numbers represent the median (range)

Phase	Group I Joints		Group II Joints	
	Responders	Non-responders	Responders	Non-responders
Soft-tissue phase				
Baseline	1.31 (0.70–7.30)	1.65 (0.55–2.95)	1.37 (0.60–5.07)	1.59 (0.71–3.67)
One-month	1.15 (0.60–4.70)	1.10 (0.50–1.70)	1.90 (1.10–3.20)	1.10 (0.50–1.90)
% Change	–28 (–61––131)	–33 (–70––118)	18 (–52–188)	–36 (–63––144)
Delayed osseous phase				
Baseline	1.19 (0.49–3.91)	1.25 (0.81–2.93)	1.46 (0.62–6.42)	1.42 (0.69–6.14)
One-month	1.00 (0.60–3.60)	1.00 (0.50–2.80)	1.20 (0.70–2.30)	1.20 (0.60–4.50)
% Change	2 (–46 to –169)	–15 (–58 to –43)	–18 (–89 to –14)	–7 (–49 to –88)

MCCR, maximum corrected count ratio.

© Quantitative Imaging in Medicine and Surgery. All rights reserved.

hand, osseous uptake was noted in 44 RA joints that were clinically unremarkable, 24 of which showed corresponding hypervascularity in soft-tissue phase. The sensitivity and specificity of clinical signs and DAS-28 have been a concern for not being able to differentiate disease activity from chronic inactive inflammation. In comparison to tools that measure vascularization like doppler ultrasound, subclinical disease is easily missed during clinical evaluation (24-26). Although the high sensitivity of this SPECT/CT method may help evaluate the disease burden, the findings should be interpreted in the clinical context (27), with emphasis on the pattern and distribution of the tracer (20).

Because soft-tissue and osseous SPECT phases reflect different pathophysiologic processes, it is not surprising to encounter discordance between the two scans. Overall, 41 joints in Group I demonstrated hypervascular soft-tissue uptake, of them 8 did not show any abnormality on the osseous phase. Isolated blood pool soft tissue hyperemia has been described for detecting RA-synovitis (12,28). On the other hand, 21/54 joints with increased osseous metabolism did not demonstrate corresponding hypervascularity. Chronic inactive arthritis can demonstrate persistent osseous uptake which limit the specificity of this finding (11,29). Alternatively, active osteitis in RA patients has been postulated to start preferentially from the bone marrow rather than the synovial membrane (inside-out theory) (4). However, it is worth mentioning that isolated osseous changes could be the result of some other pathogenic processes in the context of RA disease. For example, early bony alteration have been demonstrated using diphosphonate and were not depicted on MRI (7,11,20,30), which may reflect reactive bone repair for pre-erosive lesions. In previous studies the joints that became eroded within 2 years were scintigraphically active and showed no radiographic evidence of erosive changes at the baseline (7). A standard diagnostic CT can complement SPECT findings, provide detailed morphological evaluation of the joints, and detect more subtle alterations of the bone cortex, such as erosive changes, much earlier and more accurately compared to conventional radiography (31,32). In the context of our protocol however CT evaluation was limited by the low-dose nature of acquisition and the non-standard patient positioning.

We demonstrated the feasibility of extracting reproducible qualitative and quantitative measures of the soft tissue vascularity and osseous metabolism of both hands' joints in a single scan. This information currently may not be available by other modalities. In prior works a negative bone scan was predictive of RA treatment response and was prognostic for the absence of inflammatory joint disease for up to 3.6 years (33). This finding is highly relevant to the early identification of treatment non-responders. In our work the changes in soft-tissue phase MCCR between baseline and 1-month follow-up post-therapy seems to be generally higher compared to the delayed osseous phase MCCR. The finding of increased soft-tissue phase MCCR in Group II (osteoarthritis) joints in individual participants categorized as responders to RA therapy may be supported by recently published work (34) demonstrating that, in independent patient groups with RA and OA, both diseases showed similar disease burden at presentation to rheumatologists; however, after treatment, OA was associated with a higher mean burden of disease than RA. A recent meta-analysis showed that RA-targeted therapies may not offer clinically significant pain relief above placebo in symptomatic OA (35). In our work this rise of soft-tissue phase marker in the same patient before and after therapy for RA may reflect the fact that RA patients, who attain disease control for their RA joints after favorable response to therapy, may start to become more active and resume significant use their hands. In the absence of pain from RA joints, the mechanical sequalae may accelerate any subtle/sub-clinical osteoarthritic changes, that would be captured as an increase in the relative blood pool vascularity (21), while the delayed phase, which is driven by the lengthier process of osteoblastic modeling, would remain quiescent. The ultimate long-term objective of our work is to develop sensitive biomarkers for detecting the earliest reversible pathophysiologic changes in RA that could benefit from a specific line of treatment, like tumor necrosis factor alpha (TNF-α) blockers (36).

Our study has some merits, which include a prospective design, innovative approach for hand positioning, which allowed both hands to be imaged simultaneously, utilizing both soft-tissue and osseous-phase SPECT, and detailed analysis of observer agreement. There were also limitations. First, there was no independent validation of the results using other imaging modalities or biopsy. Second, given the pilot nature of this study, our sample size was small. Third, we did not acquire planar images for comparison with SPECT/CT; with the current experimental setup, switching between planar and SPECT/CT configurations was deemed to be logistically challenging and needed extra time. Detailed comparison between planar and tomographic scans will be carried out in future studies. Fourth, while hydration instructions were part of participant preparation

© Quantitative Imaging in Medicine and Surgery. All rights reserved.

for the scans, we were not able to ensure strict adherence to these instructions. Finally, our analysis considered each joint or joint category as independent entity and did not explicitly account for correlation between joints in the same participant.

Conclusions

Extracting reliable quantitative and qualitative measures from dual-phase ^{99m}Tc-MDP SPECT/CT of the hands is feasible in patients with RA. These measures could unleash important pathologic information on soft-tissue vascularity and bone metabolism, both of high relevance to RA assessment before and after initiation of therapy.

Acknowledgments

The authors would like to acknowledge the contributions of Drs. Piotr Maniawski from Philips Healthcare, John Brock from the University of California Davis and Dr. Angela Da Silva for helpful discussions regarding the content of the manuscript.
Funding: This work was supported in part by a research grant from Philips Healthcare and the National Institutes of Health grant number R01 AR076088. The views expressed in this article are the authors' own and do not represent the views of Philips Healthcare, or the National Institutes of Health.

Footnote

Conflicts of Interest: All authors have completed the ICMJE uniform disclosure form (available at http://dx.doi.org/10.21037/qims-20-996). Dr. RDB reports grants from Philips Healthcare, during the conduct of the study. Dr. AJC reports grants from Philips Healthcare, grants from National Institute of Health, during the conduct of the study. The other authors have no conflicts of interest to declare.

Ethical Statement: This pilot study was approved by the Institutional Review Board of the University of California Davis. Written informed consent was obtained from all study participants.

Open Access Statement: This is an Open Access article distributed in accordance with the Creative Commons Attribution-NonCommercial-NoDerivs 4.0 International License (CC BY-NC-ND 4.0), which permits the non-commercial replication and distribution of the article with the strict proviso that no changes or edits are made and the original work is properly cited (including links to both the formal publication through the relevant DOI and the license). See: https://creativecommons.org/licenses/by-nc-nd/4.0/.

References

1. Choi HJ, Lee SJ, Kim JY, Sung Y-K, Choi YY. The Correlation Between Tenosynovitis Pattern on Two-Phase Bone Scintigraphy and Clinical Manifestation in Patients with Suspected Rheumatoid Arthritis. Nucl Med Mol Imaging 2019;53:278-86.
2. Tak PP, Bresnihan B. The pathogenesis and prevention of joint damage in rheumatoid arthritis: advances from synovial biopsy and tissue analysis. Arthritis Rheum 2000;43:2619-33.
3. Takayanagi H, Oda H, Yamamoto S, Kawaguchi H, Tanaka S, Nishikawa T, Koshihara Y. A new mechanism of bone destruction in rheumatoid arthritis: synovial fibroblasts induce osteoclastogenesis. Biochem Biophys Res Commun 1997;240:279-86.
4. Schett G, Firestein GS. Mr Outside and Mr Inside: classic and alternative views on the pathogenesis of rheumatoid arthritis. Ann Rheum Dis 2010;69:787-9.
5. Mountz JM, Alavi A, Mountz JD. Emerging optical and nuclear medicine imaging methods in rheumatoid arthritis. Nat Rev Rheumatol 2012;8:719-28.
6. Van den Wyngaert T, Strobel K, Kampen WU, Kuwert T, van der Bruggen W, Mohan HK, Gnanasegaran G, Delgado-Bolton R, Weber WA, Beheshti M, Langsteger W, Giammarile F, Mottaghy FM, Paycha F, Bone E, Joint C, the Oncology C. The EANM practice guidelines for bone scintigraphy. Eur J Nucl Med Mol Imaging 2016;43:1723-38.
7. Möttönen TT, Hannonen P, Toivanen J, Rekonen A, Oka M. Value of joint scintigraphy in the prediction of erosiveness in early rheumatoid arthritis. Ann Rheum Dis 1988;47:183-9.
8. Blake GM, Park-Holohan SJ, Cook GJ, Fogelman I. Quantitative studies of bone with the use of 18F-fluoride and 99mTc-methylene diphosphonate. Semin Nucl Med 2001;31:28-49.
9. Wong KK, Piert M. Dynamic bone imaging with 99mTc-labeled diphosphonates and 18F-NaF: mechanisms and applications. J Nucl Med 2013;54:590-9.
10. Duer A, Ostergaard M, Horslev-Petersen K, Vallo J.

© Quantitative Imaging in Medicine and Surgery. All rights reserved.

Magnetic resonance imaging and bone scintigraphy in the differential diagnosis of unclassified arthritis. Ann Rheum Dis 2008;67:48-51.
11. Backhaus M, Kamradt T, Sandrock D, Loreck D, Fritz J, Wolf KJ, Raber H, Hamm B, Burmester GR, Bollow M. Arthritis of the finger joints: a comprehensive approach comparing conventional radiography, scintigraphy, ultrasound, and contrast-enhanced magnetic resonance imaging. Arthritis Rheum 1999;42:1232-45.
12. Kim JY, Choi YY, Kim CW, Sung YK, Yoo DH. Bone Scintigraphy in the Diagnosis of Rheumatoid Arthritis: Is There Additional Value of Bone Scintigraphy with Blood Pool Phase over Conventional Bone Scintigraphy? J Korean Med Sci 2016;31:502-9.
13. Buchbender C, Ostendorf B, Mattes-Gyorgy K, Miese F, Wittsack HJ, Quentin M, Specker C, Schneider M, Antoch G, Muller HW, Scherer A. Synovitis and bone inflammation in early rheumatoid arthritis: high-resolution multi-pinhole SPECT versus MRI. Diagn Interv Radiol 2013;19:20-4.
14. Ostendorf B, Scherer A, Wirrwar A, Hoppin JW, Lackas C, Schramm NU, Cohnen M, Modder U, van den Berg WB, Muller HW, Schneider M, Joosten LA. High-resolution multipinhole single-photon-emission computed tomography in experimental and human arthritis. Arthritis Rheum 2006;54:1096-104.
15. Ostendorf B, Wirrwar A, Mattes-Gyorgy K, Iking-Konert C, Blondin D, Modder U, Muller HW, Schneider M, Scherer A. High-resolution SPECT imaging of bony pathology in early arthritis of finger joints. Rheumatology (Oxford) 2009;48:853-4.
16. Aletaha D, Neogi T, Silman AJ, Funovits J, Felson DT, Bingham CO 3rd, Birnbaum NS, Burmester GR, Bykerk VP, Cohen MD, Combe B, Costenbader KH, Dougados M, Emery P, Ferraccioli G, Hazes JM, Hobbs K, Huizinga TW, Kavanaugh A, Kay J, Kvien TK, Laing T, Mease P, Menard HA, Moreland LW, Naden RL, Pincus T, Smolen JS, Stanislawska-Biernat E, Symmons D, Tak PP, Upchurch KS, Vencovsky J, Wolfe F, Hawker G. 2010 Rheumatoid arthritis classification criteria: an American College of Rheumatology/European League Against Rheumatism collaborative initiative. Arthritis Rheum 2010;62:2569-81.
17. Prevoo ML, van 't Hof MA, Kuper HH, van Leeuwen MA, van de Putte LB, van Riel PL. Modified disease activity scores that include twenty-eight-joint counts. Development and validation in a prospective longitudinal study of patients with rheumatoid arthritis. Arthritis Rheum 1995;38:44-8.
18. Colebatch AN, Edwards CJ, Ostergaard M, van der Heijde D, Balint PV, D'Agostino MA, Forslind K, Grassi W, Haavardsholm EA, Haugeberg G, Jurik AG, Landewe RB, Naredo E, O'Connor PJ, Ostendorf B, Potocki K, Schmidt WA, Smolen JS, Sokolovic S, Watt I, Conaghan PG. EULAR recommendations for the use of imaging of the joints in the clinical management of rheumatoid arthritis. Ann Rheum Dis 2013;72:804-14.
19. Huellner MW, Strobel K. Clinical applications of SPECT/CT in imaging the extremities. Eur J Nucl Med Mol Imaging 2014;41 Suppl 1:S50-8.
20. Ostendorf B, Mattes-Gyorgy K, Reichelt DC, Blondin D, Wirrwar A, Lanzman R, Muller HW, Schneider M, Modder U, Scherer A. Early detection of bony alterations in rheumatoid and erosive arthritis of finger joints with high-resolution single photon emission computed tomography, and differentiation between them. Skeletal Radiol 2010;39:55-61.
21. Abdelhafez YG, Hagge RJ, Badawi RD, Raychaudhuri SP, Chaudhari AJ. Early and Delayed 99mTc-MDP SPECT/CT Findings in Rheumatoid Arthritis and Osteoarthritis. Clin Nucl Med 2017;42:e480-1.
22. Dickson J, Ross J, Voo S. Quantitative SPECT: the time is now. EJNMMI Phys 2019;6:4.
23. De Laroche R, Simon E, Suignard N, Williams T, Henry MP, Robin P, Abgral R, Bourhis D, Salaun PY, Dubrana F, Querellou S. Clinical interest of quantitative bone SPECT-CT in the preoperative assessment of knee osteoarthritis. Medicine (Baltimore) 2018;97:e11943.
24. Bhasin S, Cheung PP. The Role of Power Doppler Ultrasonography as Disease Activity Marker in Rheumatoid Arthritis. Dis Markers 2015;2015:325909.
25. Rees JD, Pilcher J, Heron C, Kiely PD. A comparison of clinical vs ultrasound determined synovitis in rheumatoid arthritis utilizing gray-scale, power Doppler and the intravenous microbubble contrast agent 'Sono-Vue'. Rheumatology (Oxford) 2007;46:454-9.
26. Naredo E, Bonilla G, Gamero F, Uson J, Carmona L, Laffon A. Assessment of inflammatory activity in rheumatoid arthritis: a comparative study of clinical evaluation with grey scale and power Doppler ultrasonography. Ann Rheum Dis 2005;64:375-81.
27. Fisher BA, Frank JW, Taylor PC. Do Tc-99m-diphosphonate bone scans have any place in the investigation of polyarthralgia? Rheumatology (Oxford) 2007;46:1036-7.
28. Choy E. Understanding the dynamics: pathways involved

© Quantitative Imaging in Medicine and Surgery. All rights reserved.

in the pathogenesis of rheumatoid arthritis. Rheumatology 2012;51:v3-v11.
29. Zeman MN, Scott PJ. Current imaging strategies in rheumatoid arthritis. Am J Nucl Med Mol Imaging 2012;2:174-220.
30. Rosado-de-Castro PH, Lopes de Souza SA, Alexandre D, Barbosa da Fonseca LM, Gutfilen B. Rheumatoid arthritis: Nuclear Medicine state-of-the-art imaging. World J Orthop 2014;5:312-8.
31. Døhn UM, Terslev L, Szkudlarek M, Hansen MS, Hetland ML, Hansen A, Madsen OR, Hasselquist M, Moller J, Ostergaard M. Detection, scoring and volume assessment of bone erosions by ultrasonography in rheumatoid arthritis: comparison with CT. Ann Rheum Dis 2013;72:530-4.
32. Barile A, Arrigoni F, Bruno F, Guglielmi G, Zappia M, Reginelli A, Ruscitti P, Cipriani P, Giacomelli R, Brunese L, Masciocchi C. Computed Tomography and MR Imaging in Rheumatoid Arthritis. Radiol Clin North Am 2017;55:997-1007.
33. Shearman J, Esdaile J, Hawkins D, Rosenthall L. Predictive value of radionuclide joint scintigrams. Arthritis Rheum 1982;25:83-6.
34. Chua JR, Jamal S, Riad M, Castrejon I, Malfait AM, Block JA, Pincus T. Disease Burden in Osteoarthritis Is Similar to That of Rheumatoid Arthritis at Initial Rheumatology Visit and Significantly Greater Six Months Later. Arthritis Rheumatol 2019;71:1276-84.
35. Persson MSM, Sarmanova A, Doherty M, Zhang W. Conventional and biologic disease-modifying anti-rheumatic drugs for osteoarthritis: a meta-analysis of randomized controlled trials. Rheumatology (Oxford) 2018;57:1830-7.
36. Hyrich KL, Watson KD, Silman AJ, Symmons DP, British Society for Rheumatology Biologics R. Predictors of response to anti-TNF-alpha therapy among patients with rheumatoid arthritis: results from the British Society for Rheumatology Biologics Register. Rheumatology (Oxford) 2006;45:1558-65.

Cite this article as: Abdelhafez YG, Godinez F, Sood K, Hagge RJ, Boutin RD, Raychaudhuri SP, Badawi RD, Chaudhari AJ. Feasibility of dual-phase ^{99m}Tc-MDP SPECT/CT imaging in rheumatoid arthritis evaluation. Quant Imaging Med Surg 2021;11(6):2333-2343. doi: 10.21037/qims-20-996

© Quantitative Imaging in Medicine and Surgery. All rights reserved.